Schottky Heterojunction-Mediated Charge Separation in $ZnIn_2S_4$/Cu for Boosted Photocatalytic CO_2 Reduction

Honghong Xiong,[a] Haozhe Shen,[b] Yuan Cao,[b] Xu Zhang,[b] Xiang Su,[b] Ming La [b] *

[a] College of Mechanical and Electrical Engineering, Zhengzhou Shengda University, Zhengzhou, 451191, China.

[b] College of Chemistry and Chemical Engineering, Pingdingshan University, Pingdingshan, 467000, China

∗ Corresponding author. Tel.: E-mail: 2749@pdsu.edu.cn

1 Experimental Section

Sodium sulphate (Na_2SO_4), Zinc sulfate heptahydrate ($ZnSO_4 \cdot 7H_2O$), Thioacetamide (C_2H_5NS), and Copper(II) nitrate trihydrate ($Cu(NO_3)_2 \cdot 3H_2O$), and triethanolamine (TEOA) were purchased from Sinopharm Chemical Reagent Co. Ltd. (Shanghai, China). Indium (III) chloride ($InCl_3 \cdot 4H_2O$) was purchased from Aladdin Biochemical Technology Co., Ltd. (Shanghai, China). All chemicals were commercially available and used without further purification.

2 Characterization method

XRD patterns were recorded using a D8 ADVANCE X-ray diffractometer equipped with a Cu Kα radiation source (λ = 1.5406 Å), and all measurements were performed at room temperature. UV-vis DRS characterization was conducted on a Shimadzu UV-2600 spectrophotometer using barium sulfate ($BaSO_4$) as the reference substrate. XPS analysis was carried out using a Thermo Scientific ESCALAB 250XI X-ray photoelectron spectrometer, with the binding energies calibrated to the C 1s peak at 284.8 eV. transmission electron microscopy (TEM) and high-resolution TEM (HRTEM) characterization was performed using a JEOL-2010 transmission electron microscope. Surface photovoltage (SPV) responses were measured using an ESCALAB 250X photoelectron spectrometer. The Cu concentration of photocatalyst was quantified by the inductively coupled plasma optical emission spectrometry (ICP-OES, 720, Agilent). Surface photovoltage (SPV) was measured by ESCALAB 250X photoelectron spectrometer. The optical band gap of the material was calculated using the Kubelka-Munk formula, as expressed in Equation (1):

$$\alpha h\nu = A\,(h\nu - E_g)^{1/n} \qquad (1)$$

where α is the absorption coefficient, h represents Planck's constant, ν is the frequency of light, Eg denotes the band gap energy of the semiconductor, and A is a constant. The value of n depends on the

type of semiconductor: n is taken as 1/2 for a direct band gap semiconductor, while n is 2 for an indirect band gap semiconductor.

3 Photo-electrochemical measurements

Electrochemical performance measurements were conducted using a Shanghai Chenhua CHI660E electrochemical workstation with a standard three-electrode system. The working electrode was fluorine-doped tin oxide (FTO) conductive glass loaded with the catalyst, an Ag/AgCl electrode served as the reference electrode, a platinum foil was used as the counter electrode, and 0.5 $mol \cdot L^{-1}$ high-purity sodium sulfate solution was employed as the electrolyte. The working electrode was prepared as follows: 5 mg of catalyst was mixed with 250 μL of anhydrous ethanol, 250 μL of ethylene glycol, and 40 μL of 5% Nafion solution, followed by ultrasonic dispersion for 30 minutes. The loading amount was controlled at 80 $\mu L \cdot cm^{-2}$; the mixed slurry was uniformly coated onto the FTO surface to form a thin film, which was subsequently dried at 60 °C for 3 h. Transient photocurrent response tests were performed at a bias voltage of 0.6 V, and the i-t curves were recorded under alternating light/dark cycles. Electrochemical impedance spectroscopy (EIS) measurements were carried out at open circuit potential with a scanning frequency range set from 0.01 to 10^5 Hz. In the three-electrode system, the prepared sample-coated FTO served as the working electrode, a Pt electrode was used as the counter electrode, and an Ag/AgCl electrode was employed as the reference electrode.

4 Density functional theory calculations

All the density functional theory (DFT) calculations were performed by CASTEP module available in Materials Studio 7.0.[S1] The generalized-gradient approximation of Perdew-Burke-Ernzerhof (GGA-PBE) formula is used for the electronic exchange-correlation interaction. The electron wave function was expanded in plane waves with a cutoff energy of 500 eV.[S2] For the $ZnIn_2S_4$ and $ZnIn_2S_4$/Cu

supercells, the Monkhorst-Pack grid scheme k-point grid sampling were set to be 3×3×1 during the structural optimization and 5×5×1 for the electronic property calculation respectively. The total energy is converged to 1.0×10^{-5} eV/atom, and all the geometries are fully relaxed until the quantum mechanical forces acting on the atoms become less than 0.03 eV/Å.[S3] Here a thickness of 20 Å vacuum was selected in the z direction to avoid periodic interactions.

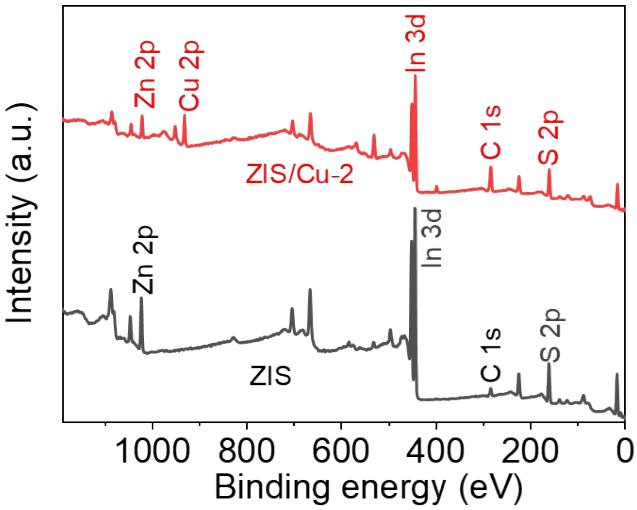

Figure S1. The survey XPS spectra of ZIS and ZIS/Cu-2.

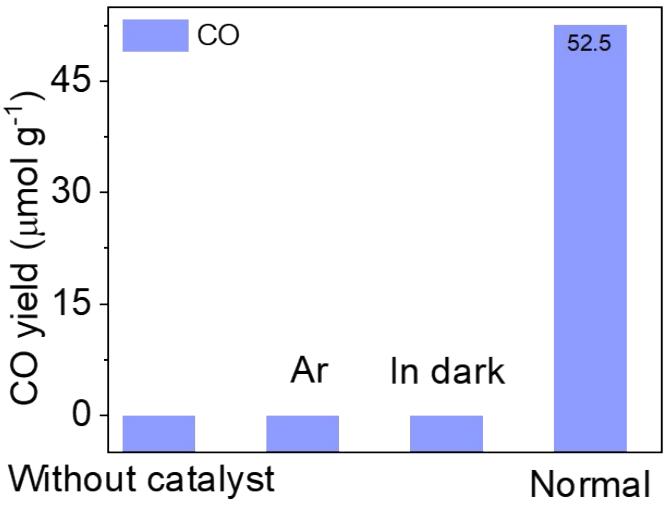

Figure S2. Evolution of CO under various reaction conditions.

Table S1. A brief list comparing the CO_2 photoreduction activity of ZIS/Cu with other reported photocatalysts.

Photocatalyst	Light source	Photocatalyst mass	Yield ($\mu mol \cdot g^{-1} \cdot h^{-1}$)	Ref.
$ZnIn_2S_4$/Cu	300 W Xe lamp	10 mg	17.5	This work
$ZnIn_2S_4$/$BiVO_4$	300 W Xe lamp	10 mg	4.75	S4
Ag/CN/$ZnIn_2S_4$	300 W Xe lamp	20 mg	5.63	S5
$Bi_4O_5I_2$@Cu-0.5	300 W Xe lamp	50 mg	7.34	S6
$ZnIn_2S_4$/MOF-808	300 W Xe lamp	50 mg	8.2	S7
Vs-$AgInS_2$	300 W Xe lamp (UVCUT 400)	20 mg	8.04	S8
TiO_2/WO_3	300 W Xe lamp	20 mg	4.73	S9
NH_2-UIO-66/COF	300W Xe lamp λ≥400 nm	10 mg	6.56	S10
g-C_3N_4/BiOCl	300 W Xe lamp	20 mg	4.73	S11
Au/Vs- $ZnIn_2S_4$	300 W Xe lamp	50 mg	8.15	S12
Co-MOF/Cu_2O	300W Xe lamp λ≥400 nm	15 mg	3.83	S13

References

S1 Fujishima A, Zhang X and Tryk D 2008 Surf. Sci. Rep., 63, 515.

S2 Perdew J P, Burke K and Ernzerhof M 1996 Phys. Rev. Lett., 77, 3865.

S3 Monkhorst H J and Pack J D 1976 Phys. Rei. B, 13, 5188.

S4 Q. Han, L. Li, W. Gao, Y. Shen, L. Wang, Y. Zhang, X. Wang, Q. Shen, Y. Xiong, Y. Zhou, Z. Zou, *ACS Appl. Mater. Interfaces,* 2021, **13,** 15092-15100.

S5 Y. Zhang, M. Gao, S. Chen, H. Wang, P. Huo, *Acta Phys. -Chim. Sin.,* 2023, **39,** 2211051.

S6 Q. Huang, J. Lin, D. Yang, Y. Hu, G. Zhou, W. Li, J. Hu, Z. Yang, *ACS Sustainable Chem. Eng.,* 2023, **11,** 17168-17178.

S7 M. Song, X. Song, X. Liu, W. Zhou, P. Huo, *Chinese J. Catal.,* 2023, **51,** 180-192.

S8 K. Wang, H. Qin, J. Li, Q. Cheng, Y. Zhu, H. Hu, J. Peng, S. Chen, G. Wang, S. Chou, S. Dou, Y. Xiao, *Appl. Catal. B-Environ. Energy,* 2023, **332,** 122763.

S9 H. Su, W. Wang, H. Jiang, L. Sun, T. Kong, Z. Lu, H. Tang, L. Wang, Q. Liu, *Inorg. Chem.,* 2022, **34,** 13608-13617.

S10 Q. Niu, S. Dong, J. Tian, G. Huang, J. Bi, L. Wu, *ACS Appl. Mater. Interface,* 2022, **14,** 24299-24308.

S11 Y. Chen, F. Wang, Y. Cao, Y. Zou, Z. Huang, L. Ye, Y. Zhou, *ACS Appl Ener Mater.,* 2020, **3,** 4610-4618.

S12 J. Lin, J. He, Q. Huang, Y. Zhang, W. Li, J. Hu, G. Zhou, Z. Yang, *Inorg. Chem.,* 2024, **63,** 13117-13126.

S13 W. Dong, J.Jia, Y. Wang, J. An, O, Yang, X. Gao, Y. Liu, J. Zhao, D. Li, *Chem. Eng. J.,* 2022, **438,**135622.